IOSR Journal of Applied Geology and Geophysics (IOSR-JAGG)
e-ISSN: 2321–0990, p-ISSN: 2321–0982. Volume 13, Issue 6 Ser. 2 (Nov – Dec 2025), PP 18-25
www.iosrjournals.org

Role Of Chamber Geometry And Crustal Heterogeneity In Stress Localization Around Pressurized Magma Chambers: Insights From Finite Element Models

Pallab Jyoti Hazarika, Mukunda Saikia
Experimental Geodynamics Laboratory, Department Of Geology, Cotton University, Guwahati-781001, India

Abstract:
Excess pressure generated within a shallow crustal magma chamber causes deformation and rupture of the chamber wall rocks and produces magma driven fractures such as dikes and inclined sheets. The regional stress field around the chamber largely controls the evolution of such dikes. The presence of mechanical heterogeneity with varying stiffness of the alternate layers can modify the patterns and magnitudes of stress localization. Thus, understanding the underlain mechanisms of stress localization around a shallow crustal magma plumbing system is essential for interpreting volcanic deformation and assessing the eruption potential. By employing a series of finite element (FE) models based on linear elasticity, the present study aims to evaluate the role of mechanical stratification and chamber geometry in governing the stress localization patterns and evolution of dikes or inclined sheets, for different excess pressure conditions. Results suggest that the configuration due to the presence of a stiff alternate layer limits the vertical propagation of tensile stress by forming a relatively uniform stress fields around the magma chambers. However, presence of an alternate compliant layer promotes vertical stress connectivity, which increases with the increasing magma excess pressure. For a circular chamber, tensile stress localizes preferentially around its boundary which is modulated by the stiffness contrast between the crustal layers. Conversely, for oblate-shaped chambers, the zones of maximum stress localization lie along its two flanks, favoring deformation and formation of inclined sheets at the chamber flanks. FE model results show that the magnitude and pattern of stress localization around a shallow magma chamber is a consequence of mutual effect of different parameters such as chamber shape, excess pressure and the presence of mechanical stratification. Thus, it is necessary to consider these diverse parameters for evaluating the deformation in a magma plumbing system at a shallow crustal depth, and to assess their eruption potential.

Key Word: *Magma plumbing system; Magma excess pressure; Young's modulus; Dike and Inclined sheets; Volcanic eruption potential.*

Date of Submission: 20-12-2025 Date of Acceptance: 30-12-2025

I. Introduction

The mechanical response of the Earth's crust to pressurization of the magma chambers plays a fundamental role in controlling a large number of inter-related processes like deformation, chamber stability, and dike initiation (Gudmundsson, 2012). Magma stored within a specific chamber exerts mechanical and thermal stress on the host rocks, which can either result in magmatic eruption or lead to magma arrest/deflection at certain depths (Gudmundsson, 2006). Thus, it is necessary to evaluate the patterns of stress localization around the chambers to understand the volcanic unrest and predict eruptive behaviour. Mechanical stratification and structural discontinuities localized in the crustal rocks can control the pathways for magma propagation styles (Clunes et al., 2021; Luppino et al., 2025; Gaffney et al., 2007). Field analyses from Santorini, Iceland, and the Central Andes, supported by numerical simulations reveal that the contrasts in layer stiffness and inclination can significantly modify local stress orientations, assisting in the deflection or arrest of dikes at the layer interfaces (Drymoni et al., 2020; Barnett & Gudmundsson, 2014; Browning & Gudmundsson, 2015; Clunes et al., 2021). Moreover, orientation of the mechanically heterogeneous layers within volcanic edifices can govern the surface stress magnitude and their locations on the surface, which can also constraint the magnitude of surface displacements (Clunes et al., 2024). Thus, existing studies emphasize the need to incorporate realistic mechanical stratification into crustal-scale models of magmatic systems.

In nature, generally the shallow crustal magma chambers have irregular shapes (Cruden and Weinberg, 2018; Gudmundsson, 2012). However, the most common shapes considered in the numerical simulations are circular and elliptical or sill-like configurations (Mogi, 1958; Gudmundsson, 2006; Browning et al., 2021; Hazarika et al., 2024). The present study considers both these geometries to examine the effect of different shapes of the magma chambers on stress localization in the surrounding host rock. The combination of chamber geometry

with varying excess pressure, and crustal stiffness conditions can clearly delineate the pathways available for magma ascent.

Existing studies on magma chamber dynamics consider a linear elastic rheology of the crustal rocks (Karaoğlu et al., 2016; Browning and Gudmundsson, 2015). Although viscoelastic or elasto-plastic behaviour are important over longer timescales or higher thermal conditions (Del Negro et al., 2009; Head et al., 2022), the short-term crustal response during inflation and unrest is dominantly elastic (Watts et al., 2013). Thus, it is necessary to consider the elastic rheology for short term deformational behaviour of the crustal rocks. Furthermore, studies combining elastic and thermal response for the crustal rocks demonstrate that thermal expansion around a magma body increases shear stress while it decreases the tensile stresses (Browning et al., 2021). These findings thus highlight the importance of thermal as well as the elastic rheological behaviour.

Despite extensive research on magma-chamber dynamics, systematic numerical analyses of stress localization due to magmatic excess pressure, for a combined variations of chamber geometry with layered crustal heterogeneity remain sparse. Existing studies consider either geometric variability (Gudmundsson, 2012; Browning et al., 2021) or stratified host rocks (Drymoni et al., 2020; Clunes et al., 2021) in isolation, rarely exploring their combined influence on stress localization around a pressurized reservoir. However, Clunes et al. (2024) have considered a combined configuration of the different magma chamber shapes along with the orientation of the mechanical layering, though the effect of the magmatic excess pressure remains mostly unexplored. This motivates our present study to examine how chamber pressurization for a different geometric configuration interacts with mechanical stratification for interpreting the deformation maps and assessing the stability of shallow magma plumbing systems. The present study addresses this gap by performing a series of finite-element simulations under a linear elastic framework. By comparing models with low and high inter-layer stiffness, we evaluate how stiffness contrast alters the magnitude and spatial extent of stress concentration zones in a layered crustal segment. We have also examined the influence of chamber geometry to evaluate the possible effect of the chamber geometry that can control the patterns and locales of the stress localization around the chamber.

II. Methodology

(i) Finite element model set-up

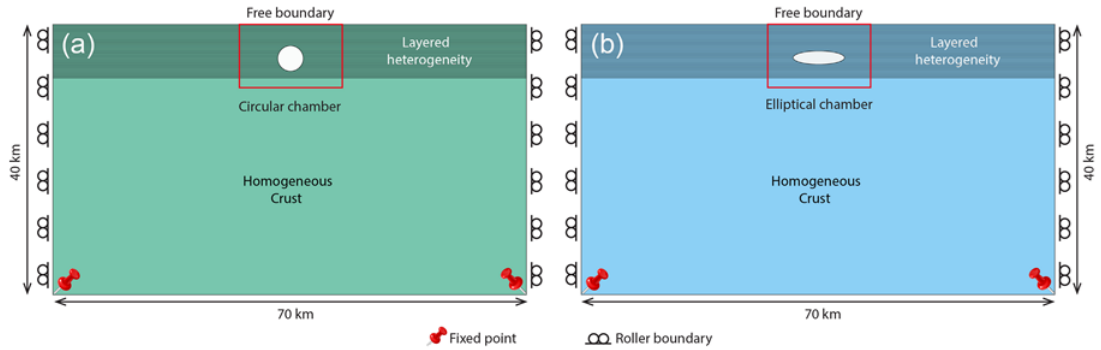

Figure 1. Schematic representation of the finite element model setup used in this study. The rectangular crustal domain (70 × 40 km) consists of a homogeneous lower crustal region and a layered upper crustal region with alternating stiffness. The magma chamber is represented as (a) a circular and (b) an elliptical cavity located at a depth of 5 km.

We designed a series of numerical models by considering a rectangular crustal segment having its horizontal extent of 70 km and depth of 40 km (Fig. 1). The homogeneous lower crust is assigned with a Young's modulus (E_1) of 40 GPa, while the upper crustal region is considered as a layered system with relatively compliant (E_2) horizontal layers of 200 m thickness. Magma chambers are represented as circular or elliptical cavities embedded within the shallow layered crust at a depth of 5 km. The circular chamber has a radius of 2 km, while the elliptical chamber is characterized by semi-major and semi-minor axes of 3 km and 800 m, respectively. The top boundary, which represents the Earth's surface, is treated as a free boundary, while both lateral boundaries are constrained with roller boundary conditions. The two bottom corners of the model domain are kept fixed to prevent any post-processing computational error.

The model domain is built with free triangular mesh elements having maximum and minimum element sizes of 2.59 km and 8.75 m, respectively. The maximum element growth rate is maintained at 1.25. A finer mesh distribution of approximately 600 elements is applied along the chamber boundary and near the top surface to reduce boundary-effects. All simulations are executed in COMSOL Multiphysics® 5.2 using the stationary MUMPS solver (Hazarika et al., 2024).

To assess the influence of mechanical layering, the stiffness of alternating shallow crustal layers is varied as E_2 = 5 GPa and E_2 = 20 GPa. For each stiffness configuration, the magma overpressure (P) is varied as 5, 6, and 7 MPa. To investigate the role of chamber geometry, these parameter variations are carried out for both circular and elliptical magma chamber configurations.

(ii) Governing equations

The finite-element formulation adopted for this study follows the linear elasticity framework used by Hazarika et al. (2024) for magma-chamber-host rock interaction. In the undeformed configuration, conservation of linear momentum for an elastic solid can be expressed as,

$$\rho \frac{\partial^2 u_i}{\partial t^2} = f_{v,i} + \frac{\partial P_{ij}}{\partial x_j} \quad (1)$$

where ρ, μ_i, $f_{v,i}$ and $\frac{\partial P_{ij}}{\partial x_j}$ are the density, displacement components, volume forces, and the Cauchy's stress tensor, respectively.

As the present study deals with time-independent deformation, inertial terms are neglected and the above equation reduces to the quasi-static balance of forces,

$$f_v + \nabla x \cdot P^T = 0 \quad (2)$$

where, P^T and f_v are the Piola Kirchoff's stress tensor and the body force vector, respectively.

The constitutive relation relates the Piola Kirchhoff's stress to the elastic strain through,

$$P^T = P_0 + P_{ext.} + C : \epsilon_{ij} \quad (3)$$

where, P_0 and $P_{ext.}$ are the reference and external stress tensors, respectively. $C = C(E, \nu)$ is the fourth-order elastic stiffness tensor, and ϵ is the strain tensor.

The infinitesimal strain tensor is expressed in terms of the displacement gradients such as,

$$\epsilon_{ij} = \frac{1}{2}\left(\frac{\partial u_i}{\partial x_j} + \frac{\partial u_j}{\partial x_i}\right) \quad (4)$$

III. Results

i) Effect of varying stiffness of the alternate layers

The influence of alternating crustal stiffness on stress localization is examined by varying the interlayer Young's modulus (E_2 = 5 and 20 GPa) under different magma excess pressure conditions (P = 5, 6 and 7 MPa) (Fig. 2, 3). For the low-stiffness configuration (E_2 = 5 GPa), the map of tensile stress localization shows pronounced intensification and propagation of tensile stresses from the chamber roof to the surface measured along the vertical direction. At P = 5 MPa, stress localization occurs primarily at the chamber boundary, which extends upward along the alternate stiff crustal layers. The tensile stress magnitude near the chamber roof reaches ~9 MPa, then it decreases upward through the inter-layered zone (Fig. 2a). Increasing the excess-pressure to 6 MPa expands the zones of high tensile stress vertically as well as laterally, forming a relatively well-connected zone of stress intensification above the chamber. At P = 6 MPa, the maximum tensile stress increases to ~11 MPa, and the zones where the stress magnitude exceeds 5 MPa become more continuous along with the inter-layered sequence within the upper layers (Fig. 2b). At P = 7 MPa, the zone of stress accumulation widens further along both vertically and laterally, producing a large, interconnected region of high stress. In this case, stress magnitudes further increase to >12 MPa near the chamber roof and 6-8 MPa extending upward towards the surface (Fig. 2c).

On the other hand, models simulated with the stiffer layered crust (i.e., E_2 = 20 GPa), stress concentration remains localized around the chamber irrespective of the choices of P. At P = 5 MPa, a narrow circular zone of stress develops adjacent to the chamber. The stress magnitude is found to be ~6 MPa near the chamber boundary that gradually decreases to ~3 MPa in the shallow crustal layers (Fig. 2d). Models solved by increasing P to 6-7 MPa, the magnitude of stress increases gradually and becomes laterally expanded, with minimum vertical stress propagation through the shallow crustal layers. At P = 6 MPa, the maximum tensile stress magnitude approaches ~8 MPa, while at 7 MPa the stress value is obtained as ~9 MPa. The reduced stiffness contrast between the alternate layers limits the vertical connectivity of stress towards the surface for a particular choice of chamber excess pressure, P (Figs. 2e-f). In summary, higher E_2 values produce a confined and stable deformation regime, whereas lower E_2 values intensifies both stress magnitude and its spatial distribution with increasing P.

ii) Effect of chamber geometry on stress localization patterns

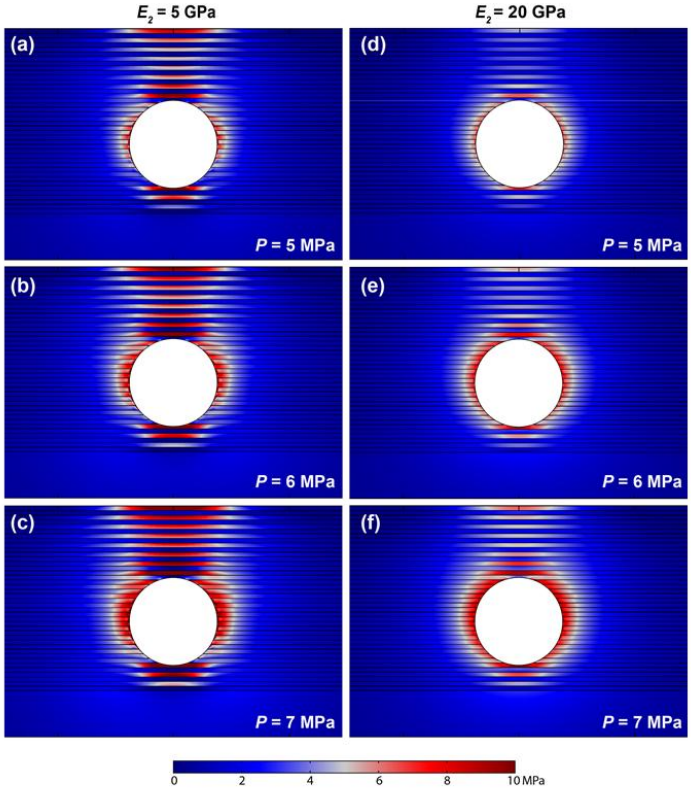

Figure 2. Tensile stress localization in a circular magma chamber embedded in a layered crustal host comprising of compliant (E_2 = 5 GPa; left panel) and stiff (E_2 = 20 GPa; right panel) inter-layer sequences for different magmatic excess pressure (P) conditions. (a, d) P = 5 MPa; (b, e) P = 6 MPa; (c, f) P = 7 MPa.

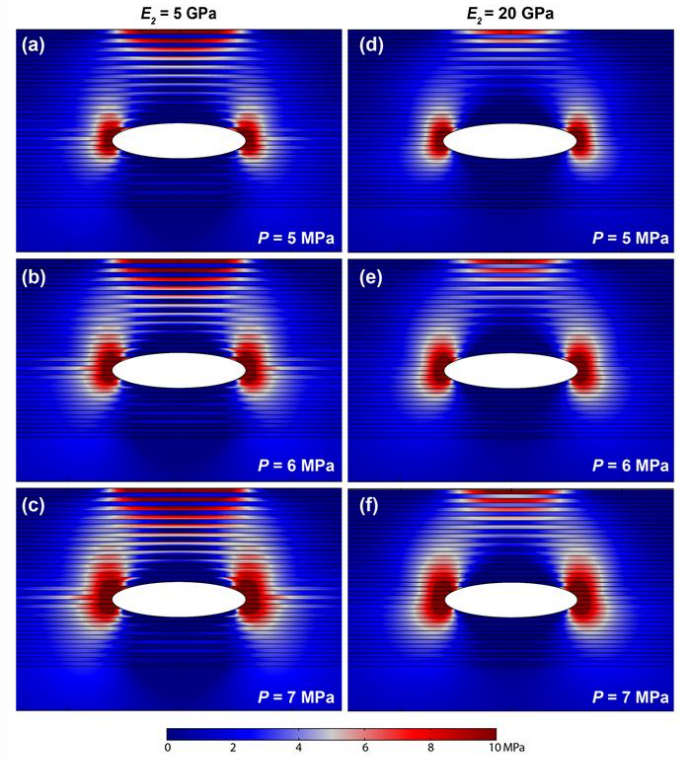

Figure 3. Tensile stress localization in an elliptical magma chamber embedded in a layered crustal host comprising of compliant (E_2 = 5 GPa; left panel) and stiff (E_2 = 20 GPa; right panel) inter-layer sequences for different magmatic excess pressure (P) conditions. (a, d) P = 5 MPa; (b, e) P = 6 MPa; (c, f) P = 7 MPa.

To investigate the potential role of chamber geometry in stress localization, a circular and an elliptical chamber configuration, embedded within a layered crustal host have been modelled by varying the excess pressure as P = 5, 6 and 7 MPa. In the models having a circular chamber geometry, the stress field is observed to be vertically symmetric and centered about the vertical axis of the chamber. For the models having compliant interlayers (E_2 = 5 GPa), at P = 5 MPa, tensile stresses are concentrated along the top and bottom of the chamber, which extend gradually towards the surface (Fig. 2a). With increasing the excess pressure (P) to 6 MPa, these zones of high tensile stress are spatially extended into the overlying layers (Fig. 2b). At P = 7 MPa, they merge into a continuous, mechanically connected vertical tensile zone extending toward the surface, indicating potential locations of roof fracturing and a favorable path for vertical dike initiation (Fig. 2c). However, the models with stiff interlayer configurations (E_2 = 20 GPa), show relatively much weaker vertical connectivity of stress between the layers for different choices of P (Figs. 2d-f).

For the elliptical chamber, the patterns and distribution of the stress field differ from those obtained with the circular magma chamber. However, it remains symmetrical about the vertical axis. For all the variations of P, the tensile stress magnitudes generate a maximum value that are obtained along the two lateral chamber tips, irrespective of the interlayer stiffness choices. For E_2 = 5 GPa, at P = 5 MPa, the average peak stress along the chamber flanks is ~15 MPa, rising to ~20 MPa at P = 6 MPa, and finally increases to ~25 MPa at P = 7 MPa (Figs. 3a-c). Similarly, for E_2 = 20 GPa, the average peak stress at P = 5 MPa is found to be ~20 MPa, which increases to ~27 MPa at P = 6 MPa, and further increases to ~32 MPa at P = 7 MPa (Figs. 3d-f). For both the considerations of interlayer stiffness (E_2 = 5 and 20 GPa), the vertical extension of the high tensile stress zones becomes prominent for a higher choice of P, which favour a strong mechanical linkage between the chamber and the near surface rock layers, forming arch-shaped stress fields above the chamber roof.

The observed differences in the stress maps obtained from our FE model results suggest that chamber shape governs the patterns of tensile stress distribution. Circular chambers promotes deformation vertically, while elliptical chambers distribute it more prominently adjacent to its lateral tips. Increasing excess pressure leads to increase in stress intensity for the two configurations of chamber geometry considered for the present analysis. However, the spatial pattern of stress localization is largely governed by the chamber shape and crustal stiffness. The most extensive and mechanically connected stress regimes occur in case of low-stiffness (E_2 = 5 GPa) and high excess pressure (P = 7 MPa) conditions, indicating the maximum potential for failure initiation in the layered crust.

IV. Discussion

(i) Stress localization in homogeneous vs. layered crust

The geometry of the volcanic edifice and the shallow magma chamber, as well as the pressure variations within the chamber has a significant control on the variation of stress field in a volcanic setting (Acocella & Neri, 2009). The tensile-stress profiles at the surface and immediately above the circular magma chamber clearly demonstrate the effect of crustal layering in modifying the patterns of stresses (Fig. 4). Such stresses induced by the magma excess-pressure can eventually contribute to the eruption dynamics. Our present study focuses on constraining the influence of stiffness of the rock layers surrounding a pressurized magma chamber. It has been demonstrated that the stiffness of host rock significantly controls the magma chamber evolution and propagation behaviour of hydro-fractures, as reported by existing studies (Gudmundsson., 2012; Barnet and Gudmundsson., 2014). For all the homogeneous and layered crustal configuration, the plots of tensile stress show a higher stress magnitude just above the chamber comparing to that of the surface stress profiles. In the homogeneous circular model (Fig. 4a), surface stress increases smoothly with magma excess pressure, with peak stress magnitudes obtained between ~3 to ~5 MPa, respectively, forming a bell-shaped profile (solid lines, Fig. 4a). Similar patterns with slightly higher magnitudes of the tensile stress (~4.5 to ~6 MPa) are also observed when the stress profiles are plotted just above the magma chamber (dotted lines, Fig. 4a). Stiff inter-layer configurations (E_2 = 20 GPa), introduce heterogeneity in the system that has substantial influence on the stress localization and results in the elevation of the above-chamber stress magnitudes to the range of ~6 to ~9 MPa (dotted lines, Fig. 4b). Similar model configuration shows that the surface stress increases relative to that of the homogeneous model to a range of ~4-6 MPa with increasing P from 5 to 7 MPa (solid lines, Fig. 4b). For the relatively compliant inter-layer case (E_2 = 5 GPa), due to the larger difference in stiffness between the alternating layers, a prominent sharpening and amplification of the stress profiles are observed (Fig. 4c). The surface stress amplifies in the range of ~8.5 MPa to ~12 MPa (solid lines, Fig. 4c), and the above-chamber stress enhances further from ~9 MPa to ~13 MPa (dotted lines, Fig. 4c) when P is increased from 5 to 7 MPa, respectively. These results suggest that the presence of an alternate sequence of stiff and compliant layers (E_2 = 5 GPa) act as effective zones for vertical stress transfer, whereas the presence of alternately lying relatively stiff layer (E_2 = 20 GPa), with a stiffer crustal rock hinders the vertical stress propagation. In other words, presence of compliant inter-layer will contribute to more extensive surface deformation in comparison to relatively stiff inter-layer configuration. These results are in agreement with previous studies (e.g., Bazargan & Gudmundsson, 2020, Clunes, 2024), that demonstrates that the presence of

mechanical contrasts can significantly modify tensile stress concentrations at the surface as well as above the circular magma chamber roof. These factors can thus influence dike propagation paths and the potential locations of eruptive vents.

For the elliptical magma chamber, stress profiles for homogeneous and layered crustal configurations are compared along the surface (solid lines, Fig. 5) and along a horizontal section across the center of the chamber (dotted lines, Fig. 5). The rationale for choosing a section across the chamber in this case is to focus on the peak stress localization along the two lateral tips of the elliptical magma chamber. The stress profiles across the chamber for both homogeneous and layered crustal configurations show higher values of stress prominently forming two peaks of equal magnitudes along the two lateral chamber tips which are directly proportional to the applied magma excess pressure (P) (dotted lines, Fig. 5). Such peak tensile stress concentration at lateral tips of the chamber indicates the zones of maximum fracturing from where dike initiates (Gudmundsson, 2006). For the homogeneous crustal case, the peak stress along the lateral tips reaches ~32 MPa and ~45 MPa for P = 5 and 7 MPa, respectively (dotted lines, Fig. 5a). However, our FE model demonstrates strong influence of crustal layering and stiffness on overall tensile stress localization for varying values of magma excess pressure. When a layered configuration is introduced in the system, the peak stress along the lateral chamber tips decreases noticeably with a prominent drop observed for the compliant inter-layer configuration. For example, a stiff inter-layer structure (E_2 = 20 GPa) produces stress magnitudes in the range of ~28 MPa to ~37 MPa, which decreases to ~20 MPa to ~30 MPa when a relatively compliant inter-layer configuration (E_2 = 5 GPa) is considered for P = 5 and 7 MPa, respectively. Existing studies have also demonstrated such patterns of peak stress localization along the two lateral chamber tips of an elliptical magma chamber (Gudmundsson, 2012; Browning & Gudmundsson, 2015; Browning et al., 2021). On the other hand, the plots of surface stress for the homogeneous as well as layered models form a Gaussian pattern with the peak stress localizing above the central region of the magma chamber. The homogeneous models show lower magnitudes of stress localization while the models with compliant inter-layer configurations show the maximum stress amplification for each of the choices of chamber excess pressure (P). For example, in case of the homogeneous models, stress magnitudes ranging from ~6 MPa to ~9 MPa (Fig. 5a) for P = 5 and 7 MPa, respectively increases to ~14 MPa to ~19 MPa for the similar choices of P (Fig. 5c).

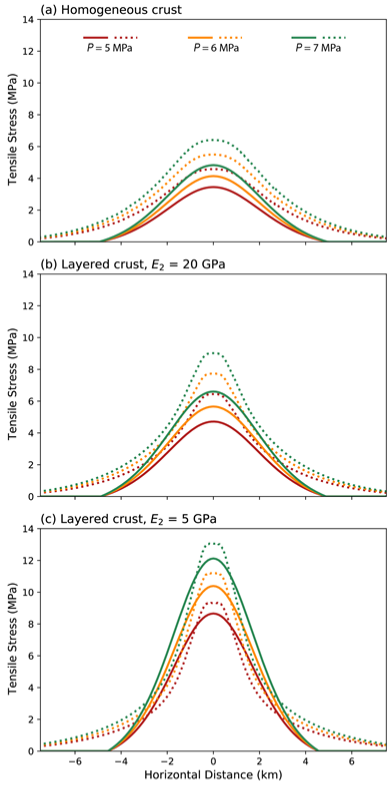

Figure 4. Comparison of the calculated tensile stress between homogeneous vs. layered crustal segment for a circular magma chamber. The solid and the dotted lines represent the evaluated stress at the surface and just above the magma chambers, respectively. (a) Homogeneous crust; (b) Layered crust with E_2 = 20 GPa; (c) Layered crust with E_2 = 5 GPa.

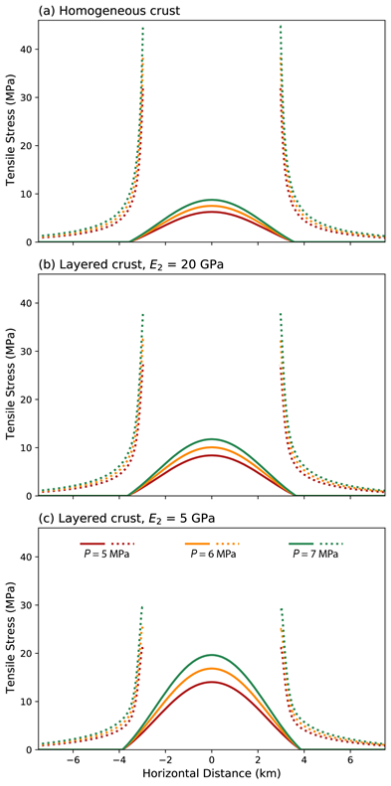

Figure 5. Comparison of stress between homogeneous vs. layered crustal segment for an elliptical magma chamber. The solid and the dotted lines represent the evaluated stress at the surface and across the center of the elliptical magma chambers, respectively. (a) Homogeneous crust; (b) Layered crust with E_2 = 20 GPa; (c) Layered crust with E_2 = 5 GPa.

(ii) Model implications

Shallow magmatic systems are commonly emplaced within mechanically layered upper-crustal region characterized by rocks with strong elastic contrasts (Gudmundsson, 2006). Such contrasts in elastic properties across layered crust causes reorientation of principal stress axes at the layer interfaces, facilitating deflection or arrest of the dike (Gudmundsson, 2011). The mechanical properties and stratification of the host rocks, as well as their geometry, depth of occurrence, and the pressure conditions of the magma chamber largely govern the state of stress within a volcanic system (Gudmundsson, 2006). A dike or sheet should propagate continuously to the surface to cause an eruption even during a volcanic unrest episode. Whether such propagation is mechanically feasible or instead results in their arrest at certain depth is governed by the local stress conditions within the volcanic edifice. Thus, it is important to note that not all the volcanic unrest episodes can cause an eruption, even when magmatic intrusions such as dikes or inclined sheets are rooted from a shallow magma reservoir (Newhall & Dzurisin, 1988; Pollard et al., 1983; Rubin, 1995; Acocella and Neri, 2003; Rivalta et al., 2005). Existing studies have reported a number of arrested dike segments exposed in volcanic fields (Geshi et al., 2010, 2012; Drymoni et al., 2020). Thus, the findings of our numerical simulations demonstrate the evolution of magmatic fractures such as dikes and inclined sheets, by using the stress maps obtained from our FE models. The in situ tensile strengths of crustal rocks average about 2-3 MPa with maximum values upto ~9 MPa (Amadei & Stephansson, 1997). The model results therefore suggest that the tensile stress magnitudes localized around the shallow magma chambers (Figs. 2, 3) are sufficient to cause deformation and initiation of inclined sheets or dikes. As stiff rocks accommodate little deformation, they tend to accumulate high tensile stresses, in contrast to compliant layers that absorb strain and limit the buildup of stress in the crustal segment (Brenner & Gudmundsson, 2004; Gudmundsson, 2011). The stress distributions obtained from the FE models performed during this study is in agreement with the aforementioned condition, where the maximum values of stress localize consistently along the stiffer layers of the layered crustal segment.

In addition, magma chamber geometry can control the pattern and orientation of principal stresses around the reservoir. Circular chambers promote vertically connected zones of tensile stress above the chamber roof, which favour the initiation of vertically propagating dikes. As discussed in a preceding section, the elliptical chambers allow tensile stresses to be concentrated near the lateral tips favouring roof failure and ring-dike development, which also agrees with existing analytical and numerical studies (Gudmundsson, 2006, 2012; Browning & Gudmundsson, 2015; Browning et al., 2021). Thus, the co-existence of mechanical stratification and a non-circular chamber geometry produces highly anisotropic stress fields, that can increase the possibility of dike deflection or arrest, and initiation of inclined sheets from the lateral tips of the chamber. Thus, our model results highlight the influence of chamber geometry and crustal mechanical layering for a range of magmatic excess pressure conditions at shallow depth range.

In summary, the numerical results obtained from this study suggest that the initiation and growth of magma driven fractures such as dikes can be controlled due to multiple physical factors such as chamber geometry, excess pressure, and the mechanical stratification of the crustal host. Therefore, it is necessary to incorporate a realistic dataset for these parameters to assess volcanic unrest signals and for evaluating the likelihood of eruption from a shallow magma plumbing system.

V. Conclusions

The present study investigates the effects of the magma chamber shape and presence of mechanical stratification on stress localization within a shallow magma plumbing system by employing a finite element modelling approach. The salient conclusions of this study are as follows:

(a) Numerical simulations presented in this study suggest that the presence of mechanical stratification in shallow crustal depths exerts a first-order control on the stress localization around pressurized magma chambers. Compliant interlayers (E_2 = 5 GPa) strongly enhance tensile stress magnitudes in the alternate stiff layers and promote a mechanical connectivity of stress between the chamber roof and the surface. Conversely, a relatively stiff inter-layered crustal host (E_2 = 20 GPa) tends to restrict stress concentration near the chamber boundary and reduce upward transfer of tensile stress towards the ground surface.

(b) Although, increasing the magma excess pressure amplifies stress magnitudes intuitively, their spatial extent around the chambers is largely controlled by the stiffness ratio between the compliant-stiff alternate layers.

(c) A circular chamber generates vertically aligned tensile stress zones above the chamber roof, favouring vertical or sub-vertical dike initiation, while an elliptical chamber accumulates stresses along its two lateral tips, favouring the development of ring-dikes or inclined sheets. However, such patterns and magnitudes of stress can be modulated by the interplay between chamber geometry, excess pressure condition as well as the presence of mechanical heterogeneity of the crust.

Acknowledgements

PJH acknowledges the INSPIRE Fellowship (IF180644) from the Department of Science & Technology, Government of India. MS acknowledges the fellowship from the CSIR-HRDG, Government of India.

References

[1]. Acocella V, Neri M. What Makes Flank Eruptions? The 2001 Etna Eruption And Its Possible Triggering Mechanisms. Bulletin Of Volcanology. 2003; 65:517–529.
[2]. Amadei B, Stephansson O. Rock Stress And Its Measurement. London: Chapman And Hall; 1997.
[3]. Barnett ZA, Gudmundsson A. Numerical Modelling Of Dykes Deflected Into Sills To Form A Magma Chamber. Journal Of Volcanology And Geothermal Research. 2014; 281:1–11.
[4]. Browning J, Gudmundsson A. Caldera Faults Capture And Deflect Inclined Sheets: An Alternative Mechanism Of Ring Dike Formation. Bulletin Of Volcanology. 2015; 77:1–13.
[5]. Browning J, Karaoğlu Ö, Bayer Ö, Turgay M, Acocella V. Stress Fields Around Magma Chambers Influenced By Elastic Thermo-Mechanical Deformation: Implications For Forecasting Chamber Failure. Bulletin Of Volcanology. 2021;83(7):1–13.
[6]. Clunes M, Browning J, Cembrano J, Marquardt C, Gudmundsson A. Crustal Folds Alter Local Stress Fields As Demonstrated By Magma Sheet–Fold Interactions In The Central Andes. Earth And Planetary Science Letters. 2021; 570:117080.
[7]. Clunes M, Browning J, Cortez J, Cembrano J, Marquardt C, Kavanagh JL, Gudmundsson A. Stresses Induced By Magma Chamber Pressurization Altered By Mechanical Layering And Layer Dip. Journal Of Geophysical Research: Solid Earth. 2024;129 (5): E2023jb027760.
[8]. Cruden AR, Weinberg RF. Mechanisms Of Magma Transport And Storage In The Lower And Middle Crust—Magma Segregation, Ascent And Emplacement. In: Volcanic And Igneous Plumbing Systems. 2018;13–53.
[9]. Del Negro C, Currenti G, Scandura D. Temperature-Dependent Viscoelastic Modeling Of Ground Deformation: Application To Etna Volcano During The 1993–1997 Inflation Period. Physics Of The Earth And Planetary Interiors. 2009;172(3):299–309.
[10]. Drymoni K, Browning J, Gudmundsson A. Dyke-Arrest Scenarios In Extensional Regimes: Insights From Field Observations And Numerical Models, Santorini, Greece. Journal Of Volcanology And Geothermal Research. 2020; 396:106854.
[11]. Gaffney ES, Damjanac B, Valentine GA. Localization Of Volcanic Activity: Effects Of Pre-Existing Structure. Earth And Planetary Science Letters. 2007;263(3–4):323–338.
[12]. Geshi N, Kusumoto S, Gudmundsson A. Geometric Difference Between Non-Feeder And Feeder Dikes. Geology. 2010; 38:195–198.
[13]. Geshi N, Kusumoto S, Gudmundsson A. Effects Of Mechanical Layering Of Host Rocks On Dike Growth And Arrest. Journal Of Volcanology And Geothermal Research. 2012;223–224:74–82.
[14]. Gudmundsson A. How Local Stresses Control Magma-Chamber Ruptures, Dyke Injections, And Eruptions In Composite Volcanoes. Earth-Science Reviews. 2006; 79:1–31.
[15]. Gudmundsson A. Magma-Chamber Geometry, Fluid Transport, Local Stresses And Rock Behavior During Collapse Caldera Formation. In: Gottsmann J, Martí J, Editors. Caldera Volcanism. Developments In Volcanology, Vol. 10. Amsterdam: Elsevier; 2008. P. 313–349.
[16]. Gudmundsson A. Rock Fractures In Geological Processes. Cambridge: Cambridge University Press; 2011.
[17]. Gudmundsson A. Magma Chambers: Formation, Local Stresses, Excess Pressures, And Compartments. Journal Of Volcanology And Geothermal Research. 2012; 237:19–41.
[18]. Hazarika PJ, Dasgupta R, Baruah A, Mandal N. Ground Surface Displacements And Stress Localization Driven By Dual Magma Chamber Dynamics: Analytical And Numerical Model Estimates. International Journal Of Earth Sciences. 2024;113(6):1475–1494.
[19]. Head M, Hickey J, Thompson J, Gottsmann J, Fournier N. Rheological Controls On Magma Reservoir Failure In A Thermo-Viscoelastic Crust. Journal Of Geophysical Research: Solid Earth. 2022;127(7):E2021jb023439.
[20]. Karaoğlu Ö, Browning J, Bazargan M, Gudmundsson A. Numerical Modelling Of Triple-Junction Tectonics At Karlıova, Eastern Turkey, With Implications For Regional Magma Transport. Earth And Planetary Science Letters. 2016; 452:157–170.
[21]. Luppino A, Bonali FL, Gudmundsson A, Tibaldi A. Effects Of Pre-Existing Fractures On Dike Propagation: New Insights From Field Data And Numerical Modelling. Journal Of Structural Geology. 2025; 105563.
[22]. Mogi K. Relation Between The Eruptions Of Various Volcanoes And Deformations Of The Ground Surfaces Around Them. Bulletin Of The Earthquake Research Institute. 1958; 36:99–134.
[23]. Newhall CG, Dzurisin D. Historical Unrest Of Large Calderas Of The World. U.S. Geological Survey Bulletin 1855. Reston, VA; 1988.
[24]. Pollard DD, Delaney PT, Duffield WA, Endo ET, Okamura AT. Surface Deformation In Volcanic Rift Zones. Tectonophysics. 1983; 94:541–584.
[25]. Rivalta E, Bottiner M, Dahm T. Buoyancy-Driven Fracture Ascent: Experiments In Layered Gelatine. Journal Of Volcanology And Geothermal Research. 2005; 144:273–285.
[26]. Rubin AM. Propagation Of Magma-Filled Cracks. Annual Review Of Earth And Planetary Sciences. 1995; 23:287–336.
[27]. Watts AB, Zhong SJ, Hunter J. The Behavior Of The Lithosphere On Seismic To Geologic Timescales. Annual Review Of Earth And Planetary Sciences. 2013; 41:443–468.